PERGAMON

Scripta mater. 42 (2000) 341–348

Scripta MATERIALIA

www.elsevier.com/locate/scriptamat

EFFECT OF AGING ON THE PHASE TRANSFORMATION AND MECHANICAL BEHAVIOR OF $Ti_{36}Ni_{49}Hf_{15}$ HIGH TEMPERATURE SHAPE MEMORY ALLOY

X.L. Meng, Y.F. Zheng, Z. Wang and L.C. Zhao

School of Materials Science and Engineering, Harbin Institute of Technology, Harbin 150001, People's Republic of China

(Received August 19, 1999)
(Accepted in revised form September 16, 1999)

Keywords: TiNiHf Alloy; Aging; Phase transformation; Mechanical behavior

Introduction

The TiNiHf alloys are newly developed as high temperature shape memory alloys with the high transformation temperatures and with lower cost in comparison with TiNiX (X = Pd, Pt) alloys. Recently a lot of investigations were focused on the TiNiHf alloys, in which Hf contents are ranged from 1% to 30% [1–8]. Zhu et al. [9] proposed that the decrease of the transformation temperatures of the $Ti_{51.5-x}Ni_{48.5}Hf_x$ (x = 15, 30) alloys in the early period of high temperature duration at 723K was due to the precipitated second phase though no further experimental results were provided. In the $Ti_{36.5}Ni_{48.5}Hf_{15}$ alloy aged at 873K for 150h, a new precipitate phase of the composition of $(Ti_{0.4}Hf_{0.6})Ni$ of a spindle-like shape with a habit plane of $(100)_P//(001)_M$ and a long axis of $[001]_P//[\bar{1}10]_M$ was observed by Han et al. [10].

It is well known that, in the Ni-rich binary TiNi SMAs, the precipitation sequences are as follows [11]:

1). β (B2 type matrix) $\rightarrow Ti_3Ni_4 \rightarrow Ti_2Ni_3 \rightarrow TiNi_3$ $\quad T \leq 953K \pm 10K$
2). $\beta \rightarrow Ti_2Ni_3 \rightarrow TiNi_3$ $\quad 953K \pm 10K \leq T \leq 1023K \pm 10K$
3). $\beta \rightarrow TiNi_3$ $\quad T \leq 1023K \pm 10K$

Until now, no results about the effects of aging at high temperature (above 953K) in the TiNiHf alloy are reported. The purpose of the present work is to investigate the microstructure, transformation temperature, mechanical properties and shape memory effects (SMEs) for $Ti_{36}Ni_{49}Hf_{15}$ alloy aged at 973K for different hours by transmission electron microscopy (TEM), X-ray diffraction (XRD) techniques, electrical resistance-temperature measurement, bending and tensile tests.

Experimental

The preparation of the experimental alloy had been described in the previous paper [4,8]. The specimens were aged at 973K for 5, 10, 20, 40, 80 and 120 hours, respectively. TEM specimens were mechanically polished to 40–50μm thick and then electrochemically polished by the twin-jet method in an electrolytic of

PII: S1359-6462(99)00347-4

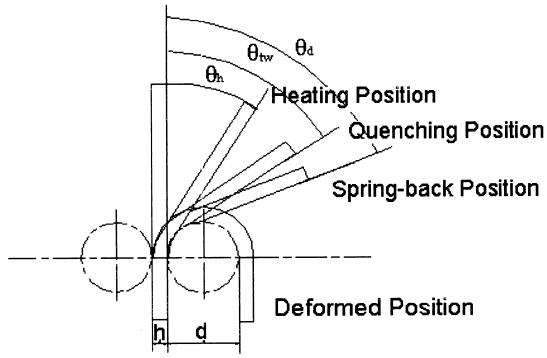

Figure 1. Schematic illustration for the SME measurement in the bending test.

20% H_2SO_4 and 80% methanol around 253K. TEM observations were performed using a JEOL-2000EX electron microscope operated at 200 kV. XRD was performed in a D/MAX-RA X-ray diffractometer.

The SME was examined by bending tests, as shown in Fig. 1. One end of the strip sample (size: 50mm × 1.5mm × 0.4mm) was clipped at the center of the plate. The specimen was bent at room temperature, and then heated up to 550K. The pre-strain, $\epsilon_t = h/(d+h)$, is about 4.2% in the present study. The recovery ratio was calculated as $R = (\theta_d - \theta_h)/\theta_d$. Subsequently, the specimens were circulated from 550K to 300K several times. At each cycle, the two-way effect was measured by the values of θ_{tw} ($\theta_{tw} = \theta_w - \theta_h$). Tensile test was conducted at ambient temperature on an Instron-1186 Model machine at a strain rate of $1.7 \times 10^{-4} \cdot S^{-1}$.

Results and Discussion

1. Microstructure of Aged $Ti_{36}Ni_{49}Hf_{15}$ Alloy

Fig. 2 illustrates the X-ray diffraction patterns of $Ti_{36}Ni_{49}Hf_{15}$ alloy aged at 973K for various hours by CuKα radiation at room temperature. The pattern can be indexed by an fcc structure $(Ti,Hf)_2Ni$ with

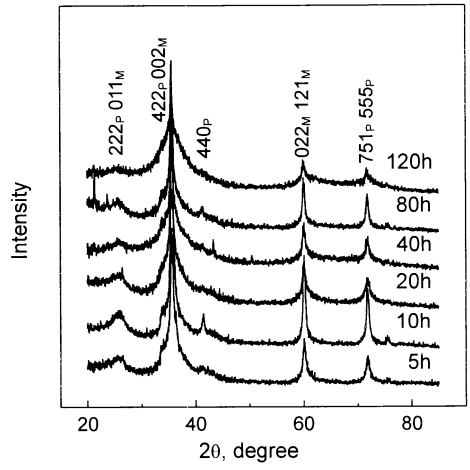

Figure 2. XRD patterns of the $Ti_{36}Ni_{49}Hf_{15}$ alloy aged at 973K for different hours.

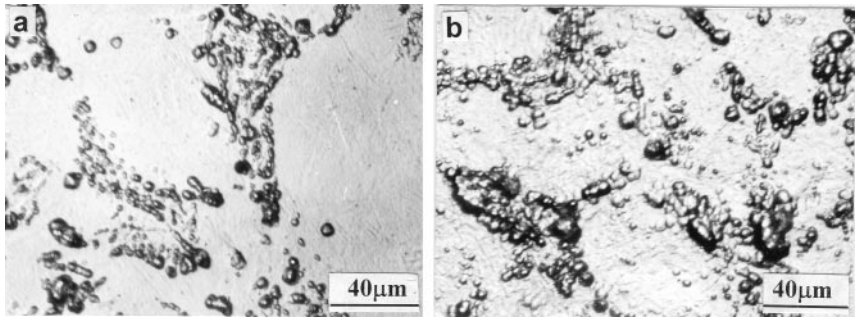

Figure 3. Optical micrographs of the $Ti_{36}Ni_{49}Hf_{15}$ alloy aged at 973K for (a) 10h; (b) 120h.

a lattice parameter of a = 1.221nm and B_{19}' type martensite of the following lattice constants: a = 0.2454nm, b = 0.4087nm, c = 0.4791nm and $\beta = 99.32°$. No new peaks are detected with the aging time increasing, which indicates that no new type of second phase precipitates during the aging. The result is similar to that in TiNiPd alloys aged at 773K for various hours [12].

The optical micrographs of the $Ti_{36}Ni_{49}Hf_{15}$ alloy aged at 973K for 10h and 120h are shown in the Fig. 3(a) and (b), respectively. It can be found that in the aged $Ti_{36}Ni_{49}Hf_{15}$ alloy most of the second particles are spherical. In the $Ti_{36}Ni_{49}Hf_{15}$ alloy aged at 973K for 10h, there are some small second phases, while in that aged for 120h, the amount of the second phases increases and the size of the second phases becomes large.

TEM observations also indicate that no new type of second phase exists in all the aging specimens, which is consistent with the results of XRD. Fig. 4(a) and (c) depict the typical morphologies of second

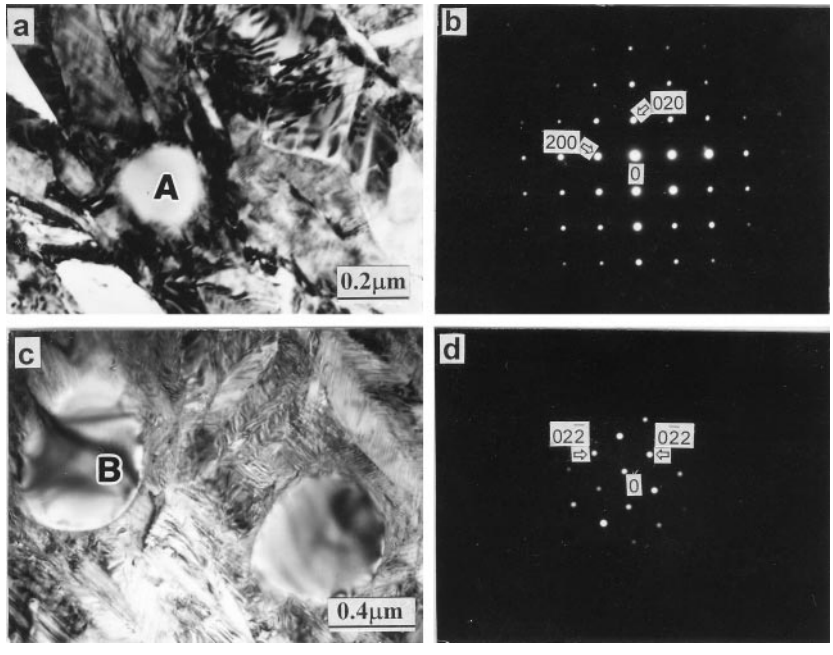

Figure 4. (a) Bright field image of $Ti_{36}Ni_{49}Hf_{15}$ alloy aged at 973K for 10h; (b) corresponding EDP of area A in (a), Electron beam // [001]; (c) Bright field image of $Ti_{36}Ni_{49}Hf_{15}$ alloy aged at 973K for 120h; (b) corresponding EDP of area B in (c), Electron beam // [111].

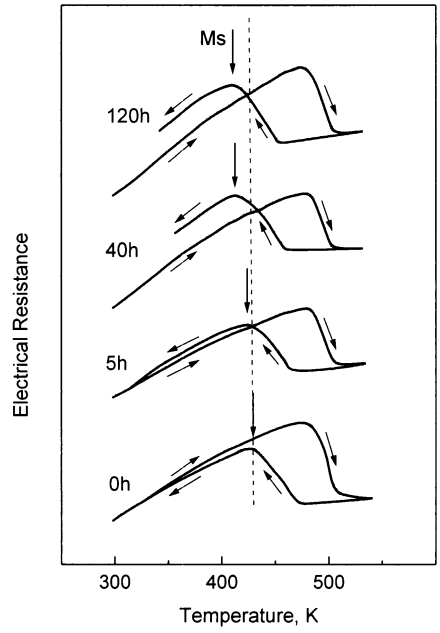

Figure 5. Electrical resistance versus temperature curves of the $Ti_{36}Ni_{49}Hf_{15}$ alloy aged at 973K for various hours.

phase particles for the $Ti_{36}Ni_{49}Hf_{15}$ alloy aged at 973K for 10h and 120h, respectively. The corresponding EDPs for the particles A and B in Fig. 4(a) and (c) are shown in Fig. 4(b) and (d). It is clear that the second phase particles are $(Ti,Hf)_2Ni$ and the size of the second phase increases with increasing aging time.

2. Effect of Aging on the Transformation Temperatures

The electrical resistance versus temperature curves of the $Ti_{36}Ni_{49}Hf_{15}$ alloys aged at 973K for 0h, 5h, 40h and 120h are shown in Fig. 5. It can be found that the shape of these curves shows no obvious changes whereas the transformation temperatures vary greatly. Fig. 6 shows the variation curves of Ms

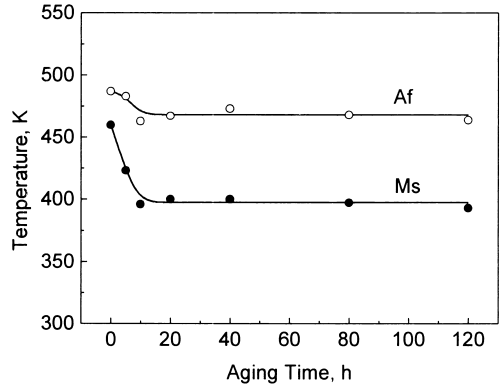

Figure 6. Effects of the aging time on the transformation temperatures Ms and Af.

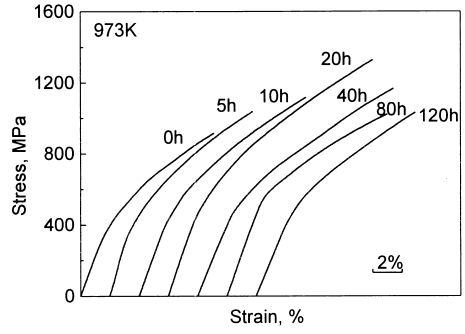

Figure 7. Stress-strain curves for the $Ti_{36}Ni_{49}Hf_{15}$ alloy aged at 973K for different hours.

and Af temperatures with the aging time. The transformation temperatures decrease rapidly with prolonging aging time at first and then keep constants as the aging time further increases.

3. Effect of Aging on the Mechanical Behavior

Fig. 7 shows the stress-strain curves at ambient temperature of the specimen aged at 973K for different hours. Unlike that of annealed TiNi alloys [13], no stress plateau is observed. The stress-strain curves are characterized by continuous yielding and high work-hardening, which is similar to that of TiNiPd [14], cold-worked TiNi alloys [15] and solution-treated $Ti_{36}Ni_{49}Hf_{15}$ alloys [16]. The high work hardening probably results from some defects introduced during the martensite variant reorientation or the stress induced martensitic transformation. The yield strength and the elongation change a little as the aging time increases from 0h to 120h, as shown in Fig. 8. It is clear that the yield strength of the specimen reaches a weak peak value when the aging time is about 20h and then slightly decreases. The elongation of the aged specimen changes slightly as the aging time further increases and then decreases rapidly when the aging time exceeds 80h. There is no apparent hardening in $Ti_{36}Ni_{49}Hf_{15}$ alloy aged at 973K.

4. Effect of Aging on the Shape Memory Effect

The SME of the alloy changes with increasing aging time. The shape recovery ratio of the $Ti_{36}Ni_{49}Hf_{15}$ alloy is shown in Fig. 9 as a function of the aging time. The recovery ratio increases with increasing

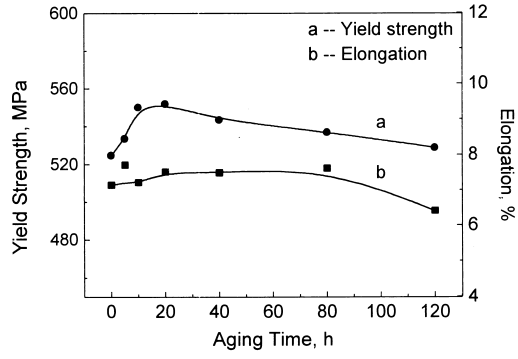

Figure 8. Effect of the aging time on the yield strength and the elongation.

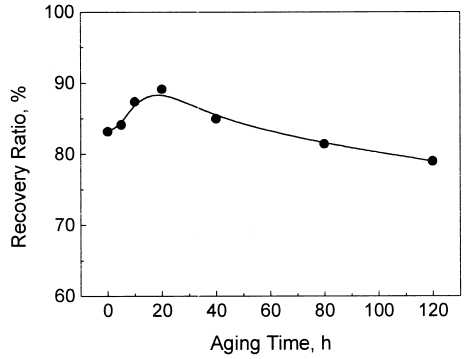

Figure 9. Effect of the aging time on the shape recovery ratio.

aging time, and reaches a maximum at about 20h, then decreases slowly. The maximum recovery ratio is about 90%, which is lower than that of hot-rolled and annealed $Ti_{36}Ni_{49}Hf_{15}$ alloy [16].

For the TiNiHf alloys, no two-way shape memory effect (TWSME) was reported in the previous literatures. However, obvious TWSMEs both in the solution-treated and in the aged $Ti_{36}Ni_{49}Hf_{15}$ alloy are observed in the present study. The TWSME in the aged $Ti_{36}Ni_{49}Hf_{15}$ alloy is unstable, and decreases as the number of cycles increases, which is similar to that in TiNi alloys [17]. The curve of θ_{tw} with the aging time and the number of cycles are plotted in Fig. 10. It is apparent that θ_{tw} decreases rapidly at the first several cycles, then decreases slowly as the number of cycles increases, finally reaches a saturation value. The phenomenon may be explained by a change in the dislocation pattern [17]. It is well known that the TWSME originates from the complex dislocation arrays caused by bending deformation. These dislocations form a stress field that is beneficial to the forward and reverse transformations of preferentially oriented martensites under thermal cycles. Perhaps the second phase particles grown up during the aging interact with the dislocations, which deteriorates the TWSME.

Although no new kinds of precipitate particles are observed in the $Ti_{36}Ni_{49}Hf_{15}$ alloy after aging at 973K, the aging affects the transformation temperatures, the mechanical properties and the SME of the alloy. The further precipitation of $(Ti,Hf)_2Ni$ and the coarsening of original $(Ti,Hf)_2Ni$ maybe occur during the aging, which results in the change of matrix composition (or (Ti+Hf)/Ni atomic ratio). The decrease of the transformation temperatures can be attributed to the change of composition (or (Ti+Hf)/Ni atomic ratio) in the matrix, especially in the change of Hf content in the matrix.

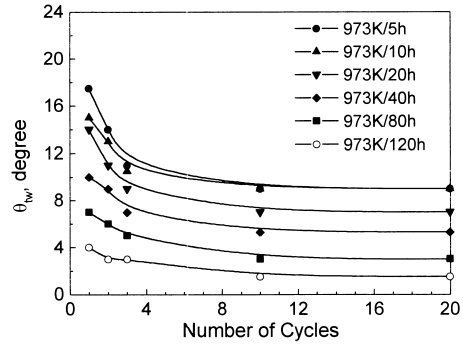

Figure 10. Effect of the aging time and the number of cycles on the TWSME.

The experimental results suggest that some $(Ti,Hf)_2Ni$ particles freshly precipitated at the beginning of the aging. With increasing aging time, all $(Ti,Hf)_2Ni$ particles including preexisted ones coarsen, which affects the mechanical properties and SME of the alloy. When the aging time is less than 20h, the precipitated small particles strengthen the matrix slightly, which results in the slight increase of the yield strength of the alloy. In addition, these particles increase the SME of the alloy by reacting with the dislocations. With further increasing the aging time, the coarsening of the second phase particles leads to the decrease of the strength and SME of the alloy.

Obvious TWSME is observed in the present alloy. After several thermal cycles, the TWSME decreases probably because the stress field introduced by dislocations relaxes, or in other word, the dislocations rearrange. The fact that, with increasing aging time, the TWSME is deteriorated may be explained by the effect of second phase particles.

All in all, no new fine second phase was observed in the $Ti_{36}Ni_{49}Hf_{15}$ alloy aged at 973K for various hours. The process of aging maybe includes the precipitation of fresh $(Ti,Hf)_2Ni$ particles and the growth up of preexisted ones. As a result, the mechanical properties and SME change correspondingly with increasing aging time.

Conclusions

1. No new kinds of precipitate particles are observed in the $Ti_{36}Ni_{49}Hf_{15}$ alloy but $(Ti,Hf)_2Ni$ during aging at 973K.
2. The transformation temperatures of the $Ti_{36}Ni_{49}Hf_{15}$ alloy decrease rapidly with prolonging aging time at first and then keep constants as the aging time further increases.
3. The yield strength reaches the maximum when the alloy was aged at 973K for about 20 hours. Whereas the elongation almost keeps constant at first and then decreases rapidly when the aging time exceeds 80 hours. No obvious age hardening was found in the $Ti_{36}Ni_{49}Hf_{15}$ alloy aged at 973K.
4. With increasing aging time, a weak peak of SME of aged alloy is observed when the aging time is about 20 hours.
5. An obvious TWSME is observed in the $Ti_{36}Ni_{49}Hf_{15}$ alloy, which is deteriorated with increasing aging time. After several thermal cycles, the TWSME decreases.

References

1. K. H. Wu and Z. J. Pu, J. Phys. IV. C8, 801 (1995).
2. D. R. Angst, P. E. Thoma, and M. Y. Kao, J. Phys. IV. C8, 747 (1995).
3. P. Olier, J. C. Brachet, J. L. Bechade, C. Foucher, and G. Guenin, J. Phys. IV. C8, 741 (1995).
4. Y. F. Zheng, W. Cai, J. X. Zhang, Y. Q. Wang, L. C. Zhao, and H. Q. Ye, Mater. Lett. 36, 142 (1998).
5. X. D. Han, W. H. Zou, R. Wang. Z. Zhang, and D. Z. Yang, Acta Mater. 44, 3711 (1996).
6. P. L. Potapov, A. V. Shelyakov, A. A. Gulyaev, E. L. Svistunova, N. M. Matveeva, and D. Hodgson, Mater. Lett. 32, 247 (1997).
7. X. D. Han, Z. F. Zhang, T. C. Li, J. T. Liu, and D. Z. Yang, in Proceedings of the International Symposium on Shape Memory Materials, ed. C. Youyi and T. Hailing, p. 258, International Organization on SMM (1994).
8. Y. F. Zheng, L. C. Zhao, and H. Q. Ye, Scripta Mater. 38, 1249 (1998).
9. Y. R. Zhu, Z. J. Pu, C. Li, and K. H. Wu, in Proceedings of the International Symposium on Shape Memory Materials, ed. C. Youyi and T. Hailing, p. 253, International Organization on SMM (1994).
10. X. D. Han, R. Wang, Z. Zhang, and D. Z. Yang, Acta Mater. 46, 273 (1998).
11. M. Nishida, C. M. Wayman, and T. Honma, Metall. Trans. 17, 1505 (1986).
12. H. Xu, Q. Meng, C. Jiang, and S. Gong, in Proceedings of the Third Pacific Rim International Conference on Advanced Materials and Processing, ed. M. A. Imam, R. DeNale, S. Hanada, Z. Zhong, and D. N. Lee, p. 2039, The Minerals, Metals & Materials Society, Warrendale, PA (1998).

13. S. Eucken and T. W. Duerig, Acta Metall. 37, 2245 (1989).
14. D. Golberg, Y. Xu, Y. Murakami, S. Morito, and K. Otsuka, Scripta Metall. Mater. 30, 1349 (1994).
15. H. C. Lin and S. K. Wu, Acta Metall. 42, 1623 (1994).
16. Y. Q. Wang, Y. F. Zheng, W. Cai, and L. C. Zhao, Scripta Mater. 40, 1327 (1999).
17. H. Scherngell and A. C. Kneissl, Scripta Mater. 39, 205 (1998).